

*Original Research*

# Study on the Preparation of Hydrogen-Rich Fuel Gas from Mixed Pyrolysis of Coal by Alkaline Earth Metal Oxide Supported $\gamma$ -Al<sub>2</sub>O<sub>3</sub> Catalyst

Chen Jihao<sup>1,2,3\*</sup>, Xia Fei<sup>1,3</sup>, Li Yue<sup>1,2,3</sup>, Li Juan<sup>1,3</sup>, Tong Meng<sup>1,3</sup>

<sup>1</sup>Shaanxi Coal Geological Engineering Technology Co., Ltd., Xi'an 710054, China

<sup>2</sup>Key Laboratory of Coal Resources Exploration and Comprehensive Utilization, Ministry of Natural Resources, Xi'an, 710021, China

<sup>3</sup>Shaanxi Coal Geological Laboratory Co., Ltd., Xi'an, 710054, China

*Received: 3 April 2021*

*Accepted: 10 September 2021*

## Abstract

In this experiment,  $\gamma$ -Al<sub>2</sub>O<sub>3</sub> was used as the carrier, and the alkaline earth metal oxide supported  $\gamma$ -Al<sub>2</sub>O<sub>3</sub> catalyst was prepared by an equal volume impregnation method. The coal sample and the catalyst were mixed and pyrolyzed through a fixed pyrolysis bed to produce hydrogen-rich fuel gas and tar. The effects of pyrolysis conditions on hydrogen rich fuel gas components and tar were studied by changing the final pyrolysis temperature (450°C, 500°C, 550°C, and 600°C) and constant pyrolysis time (3 min, 5 min, 10 min and 15 min); MgO, CaO, SrO and BaO were used as active components, and the alkaline earth metal oxide supported  $\gamma$ -Al<sub>2</sub>O<sub>3</sub> catalyst was prepared and roasted by muffle furnace, and then the effects of alkaline earth metal oxides on hydrogen rich fuel gas components and tar were studied. The catalyst was characterized by XRD and BET, and the pyrolysis mechanism of coal and catalyst was studied. The results show that: (1) When the final temperature was 600°C, the maximum tar was 0.32g, and the maximum gas was 1.44g. The CH<sub>4</sub> content was the largest from 450°C to 550°C, and the hydrogen content was the maximum at 600°C. (2) The content of hydrogen at the final temperature 600°C was the highest, and the oil yield was basically unchanged. (3) SrO/ $\gamma$ -Al<sub>2</sub>O<sub>3</sub> and BaO/ $\gamma$ -Al<sub>2</sub>O<sub>3</sub> catalyst had a good effect on coal pyrolysis to produce hydrogen rich fuel gas. (4) The specific surface areas of  $\gamma$ -Al<sub>2</sub>O<sub>3</sub> and BaO/ $\gamma$ -Al<sub>2</sub>O<sub>3</sub> were similar, but the XRD characterization showed that the BaO/ $\gamma$ -Al<sub>2</sub>O<sub>3</sub> catalyst contained more BaO active components, so BaO/ $\gamma$ -Al<sub>2</sub>O<sub>3</sub> has better catalytic cracking effect.

**Keywords:** alkaline earth metal oxide,  $\gamma$ -Al<sub>2</sub>O<sub>3</sub>, mixed pyrolysis, hydrogen rich fuel gas, tar

## Introduction

The clean utilization of coal is to convert coal into a wide range of clean energy through pyrolysis that does little harm to the environment and human body [1]. Coal is pyrolyzed to produce tar, pyrolysis gas, and coke [2]. Tar is used to make power fuel oil and refined into gasoline and diesel blended oil. It can also be used to refine more chemical products from coal tar. Pyrolysis gas contains more fuel gas, such as hydrogen, methane, carbon monoxide and other combustible gases [3], which can be used as industrial fuel combustion for power generation and city gas to improve the utilization efficiency of coal. At the same time, the coke produced can also be used as fuel combustion for power generation, heat generation and heating. The extensive utilization of tar, pyrolysis gas and coke greatly improves the comprehensive utilization efficiency of coal, and gradually reflects huge economic value, which is of great significance to the efficient use of energy and environmental protection [4].

The low-temperature carbonization of coal is simpler than coal gasification and liquefaction, with mild processing conditions, simple production equipment, and less investment [5]. Temperature is one of the important factors affecting coal pyrolysis, and it has a great influence on the secondary reactions that generate primary pyrolysis products and volatiles. Pyrolysis temperature has a great influence on the pyrolysis characteristics and secondary reactions of coal [6], and the secondary reactions hardly exist below 600°C [7]. Volatile components will not undergo cracking and re-polymerization. The tar yield was higher in this temperature section, and the yield of semi-coke and pyrolysis gas was lower. When the temperature was above 600°C, the secondary reaction was intensified, and the primary volatile was cracked and repolymerized, and part of tar was cracked into gas, resulting in the decrease of tar yield and the increase of semi-coke and gas yield. The residence time of gaseous products (gas and tar) and solid products (semi coke) in the pyrolysis zone had an effect on the final pyrolysis products. With the increase of residence time, the yield of tar decreased, while the yield of pyrolysis gas products and light hydrocarbons increased, and the component distribution and content of tar changed [8]. The effect of gas residence time on pyrolysis reaction during coal pyrolysis is important [9]. The experiment found that with the increase of residence time, the yield of pyrolysis gas increased significantly, the yield of tar increased first and then decreased, the residual volatile matter in solid char decreased, and the H/C decreased. Compared with the secondary bituminous coal and lignite, the tar produced by bituminous coal pyrolysis was more, and the hydrocarbon gas, water and CO<sub>2</sub> were less.

The yield of tar and pyrolysis gas produced by direct pyrolysis of coal was low, the quality is poor and the

utilization rate was low. Therefore, adding catalyst in the pyrolysis process played an important role in improving the yield and quality of tar and pyrolysis gas, but the selection of catalyst determined the yield and quality of coal pyrolysis products. Liu The catalytic pyrolysis of coking coal tail coal to produce hydrogen rich fuel gas, and found that in the catalytic pyrolysis experiment, CaO promoted the production of H<sub>2</sub> from tail coal pyrolysis, except that Al and MgO inhibited the pyrolysis of tail coal [10]. The effect of CaO on the distribution of pyrolysis products and char structure of lignite and anthracite [11]. The results showed that the cumulative H<sub>2</sub> yield of lignite coal with 2% CaO was the largest, reaching 39.11ml/g; the cumulative yield of CO generated by coal sample with CaO at high temperature pyrolysis stage was greater than that of coal without CaO. Jiao Yi [12] prepared catalysts for the cracking of kerosene with BaO and SrO as active components, and found that the addition of BaO or SrO as active components effectively inhibited carbon deposition, and the synergistic effect of BaO or SrO additives enhanced the cracking reaction. Therefore, it can be found that alkaline earth metal oxides had different degrees of catalytic effect on coal pyrolysis.

In this study,  $\gamma$ -Al<sub>2</sub>O<sub>3</sub> was used as the carrier to prepare the catalyst, because of its excellent physical and chemical properties, it was very suitable for experimental operation and industrial application. At the same time, alkaline earth metal oxides were loaded into  $\gamma$ -Al<sub>2</sub>O<sub>3</sub> to prepare supported catalysts, and their effects on oil and gas production during coal pyrolysis were studied, a supported  $\gamma$ -Al<sub>2</sub>O<sub>3</sub> catalyst with high catalytic efficiency was prepared to improve the yield and quality of hydrogen-rich fuel gas during coal pyrolysis.

## Material and Methods

### Materials and Drugs

The coal used in the experiment was produced in Cuimu Coal Mine, Shaanxi, with a particle size of 3~5 mm. Table 1 shows the results of industrial analysis and elemental analysis of the coal sample.  $\gamma$ -Al<sub>2</sub>O<sub>3</sub> was purchased on the market with a particle size of 3~5mm. MgCl<sub>2</sub>, CaCl<sub>2</sub>, SrCl<sub>2</sub> and BaCl<sub>2</sub> were all analytically pure.

### Preparation of Catalysts

By constant volume impregnation, 3 g  $\gamma$ -Al<sub>2</sub>O<sub>3</sub> was immersed in 5% MgCl<sub>2</sub> solution for 24 h. It was taken out and placed in a muffle furnace and roasted at 450°C for 4 h. It was removed as MgO/ $\gamma$ -Al<sub>2</sub>O<sub>3</sub> catalyst with 5% loading. CaO/ $\gamma$ -Al<sub>2</sub>O<sub>3</sub>, SrO/ $\gamma$ -Al<sub>2</sub>O<sub>3</sub> and BaO/ $\gamma$ -Al<sub>2</sub>O<sub>3</sub> catalysts with 5% loading were prepared by the same method.

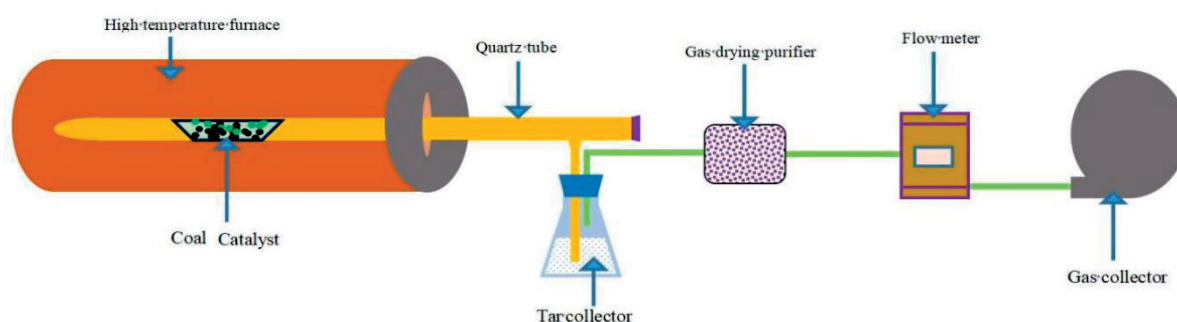


Fig. 1. Reaction device diagram.

### Activity Evaluation of Catalyst

In the experiment, in the coal pyrolysis cracking catalytic system, 15 g coal sample and 3 g catalyst were mixed and placed at furnace was vacant. First, the coal undergoes a catalytic pyrolysis reaction, and the resulting pyrolysis product entered the tar collector. The liquid phase components of the catalytic pyrolysis were collected, and the gas phase components were dried. The gas was collected and detected by the gas collector. The dried gas entered the flowmeter to count the volume, and then it was collected and detected. At the end of the experiment, the tar attached in the reaction tube and condensation tube was washed with acetone, and all acetone solutions containing tar were collected together. The water in tar was collected by anhydrous sodium sulfate, and then the acetone was removed by rotary evaporation, and the tar was collected and weighed. The gas components were detected by gas chromatography, and the changes of gas and tar components were analyzed. In this paper, the effect of catalyst was evaluated by the change of pyrolysis products of bituminous coal.

### Detection of Pyrolysis Products of Coal Tar

The gas produced by catalytic cracking of tar was collected by gas collecting bag and analyzed by GC-2014c gas chromatography. The working conditions of gas chromatography were shown in Table 2 below.

### Characterization

Thermogravimetric analysis of the raw coal: the raw coal was a Swiss Mettler-Toledo TGA/SDTA851e thermogravimetric analyzer. During the experiment, the carrier gas was selected from high purity  $N_2$ , the gas flow rate was 60 mL/min, the temperature range was 24°C~500°C, and the heating rate was 15°C/min.

Specific surface area (BET): The JW-BK122W type surface and pore size analyzer is used to measure the specific surface area of different types of the catalysts.

X-ray analysis (XRD, Beijing General Analysis Instrument Co., Ltd.): XD-3 type ray diffractometer; the test parameters: the voltage is 36 KV, the current is 20 mA, the target is Cu, K alpha rays,  $2\theta/\theta$  is 5° to 80°, and scanning speed is 4(°)/min.

Table 1. Industrial analysis and elemental analysis of coal samples (%).

Industrial analysis/%				Elemental analysis/%				
Mad	Aad	Vad	FCad	C	H	O	N	S
4.99	11.87	32.79	50.35	62.22	3.720	12.28	0.89	1.18

Table 2. Operating conditions of GC,

Detector	TCD	FID
Column type	Packed column	Packed column
Gasification chamber temperature (°C)	360	360
Column box temperature (°C)	80	80
Detector temperature (°C)	100	150
Determination of gases	$CO_2, H_2, N_2, CO, O_2$	$CH_4, C_2H_6, C_3H_8, C_4-C_8$

Inductively coupled plasma mass spectrometer (ICP-MS): iCAP Q type, (Thermo Fisher Scientific, USA), working conditions, RF generator power: 1400 kw, cooling gas flow rate: 13.0 L/min, auxiliary gas flow rate: 0.72 L/min, scanning mode: peak jump, atomizer flow rate: 0.90 L/min, sampling time: 20s, sampling pump speed: 70 rpm, sampling depth: 150 mm, sampling cone: 1.1 mm, intercepting cone: 0.9 mm, double charge production Rate:  $IBa^{++}/Ba < 3\%$ , oxide yield,  $ICeO+/Ce < 3\%$ , mainly used to determine the content of catalysts.

## Results and Discussion

### Effect of Final Pyrolysis Temperature on Coal Pyrolysis Products

Fig. 2 showed the changes of gas products and tar when 15 g coal was put into the pyrolysis furnace at the final temperature of 450°C, 500°C, 550°C and 600°C. With the increase of pyrolysis temperature, the quality of gas products and tar was also increasing. The pyrolysis of coal can be roughly divided into three stages [13]. The first stage was drying and degassing from room temperature to 350°C, mainly physical changed. The second stage was from 350°C to 550°C, mainly depolymerization and decomposition, and a large amount of volatile gas and tar were generated, which was also the process of coal coking. The third stage was from 550°C to 1000°C, and the secondary degassing was mainly polycondensation, which produced less tar. The volatile components were mainly hydrocarbon gas, hydrogen and carbon oxides. This experiment was mainly to study the second stage of coal pyrolysis. When the temperature was 450°C, the tar was 0.19 g and the gas yield was 0.60 g. When the final temperature was 600°C, the tar was 0.32g, and the gas

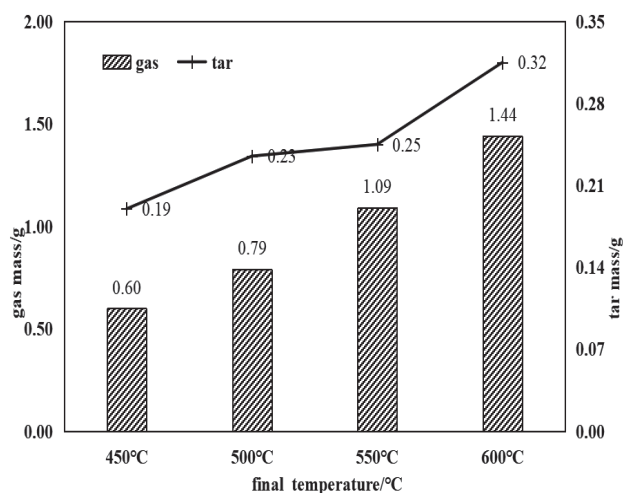


Fig. 2. Effect of final pyrolysis temperature on pyrolysis gas and tar.

production was 1.44g. The tar and gas production were increased by 68.4% and 140% respectively compared with that at 450°C. Because 600°C was in the third stage of coal pyrolysis, the amount of gas produced by polycondensation increased obviously, which means that the amount of tar at this stage was the maximum, and which was the best temperature to study coal tar pyrolysis.

Fig. 3 showed the change of gas composition at different final temperature during coal pyrolysis. The main components of pyrolytic gas were  $CO_2$ , CO,  $H_2$ ,  $CH_4$ ,  $C_2$ ,  $C_3$  and  $C_4\sim C_8$ . As the temperature increased, the content of each gas component increased first and then decreased. However, the maximum content of each gas component occurs at different temperatures, the highest temperatures of  $CO_2$ , CO,  $H_2$ ,  $CH_4$ ,  $C_2$ ,  $C_3$  and  $C_4\sim C_8$  were 400°C, 500°C, 550°C, 500°C, 450°C, 400°C and 400°C respectively. The content of  $H_2$  and  $CH_4$  in coal pyrolysis gas was higher, the content of  $CO_2$  and CO was lower, and the content of other gas was lowest. The content of CO,  $H_2$  and  $CH_4$ , as well as the content of  $H_2$  and  $CH_4$  were the main factors to use coal pyrolysis gas as hydrogen-rich fuel gas. The maximum contents of CO,  $H_2$  and  $CH_4$  and the content of  $H_2$  and  $CH_4$  were 71.3% and 61.3% respectively when the final pyrolysis temperature was 550°C. The temperature range from 400°C to 550°C was the second temperature range of coal pyrolysis, in which a large amount of coal pyrolysis gas and oil were produced, and the content of  $CH_4$  was the largest at each final temperature point. When the temperature reached 600°C, the content of  $H_2$  increased and exceeded the content of  $CH_4$ . The main reason was that 600°C was in the third temperature range, and the volatiles was mainly hydrocarbon gases, hydrogen and carbon oxides, so the content of  $H_2$  increased and reached 21.6%.

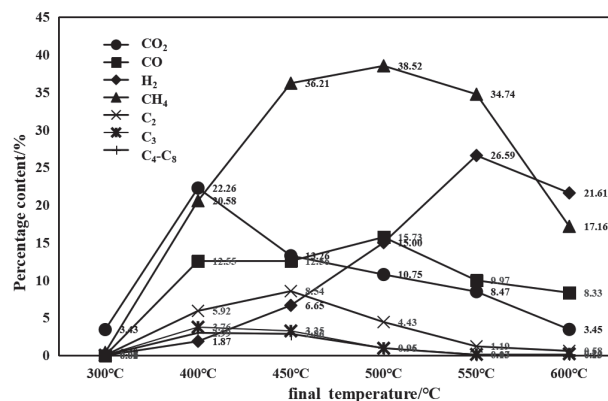


Fig. 3. Effect of final pyrolysis temperature on gas composition of coal pyrolysis.



### Effect of Constant Temperature Time on Pyrolysis Products

Fig. 4 was the change of gas products and tar at constant temperature for 3 min, 5 min, 10 min and 15min at final pyrolysis temperature 600°C. As can be seen from Fig. 4, when the final pyrolysis temperature was 600°C, the gas yield and tar yield increased with the increase of pyrolysis time, but the increase trend was slow. The tar was 0.32 g at 3 min, and the tar was 0.37 g at 15 min. The yield of tar were 15.63% higher at 15 min than that the final pyrolysis temperature 600°C. However, the output of pyrolysis gas had been increasing. Because the final temperature of pyrolysis was 600°C in the third stage of coal pyrolysis, the secondary degassing was mainly polycondensation, which produced less tar, and the volatiles were mainly hydrocarbons. As a result, the gas production had been increasing, and the oil product had increased less. Compared with the final temperature 600°C, the gas production increased by 17.4%. Therefore, it can be proved that the final temperature was 600°C and the oil in coal was basically pyrolyzed, and the gas production was increased due to polycondensation reaction.

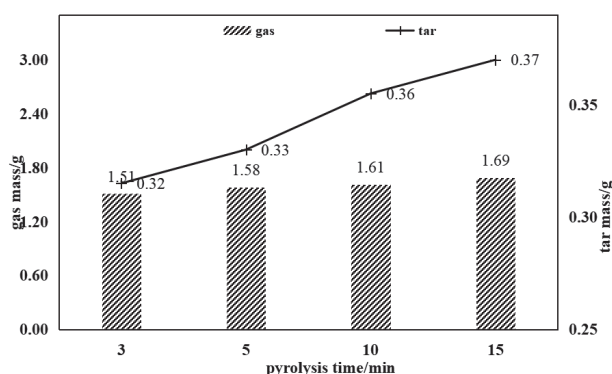


Fig. 4. Effect of constant temperature time on pyrolysis gas and tar.

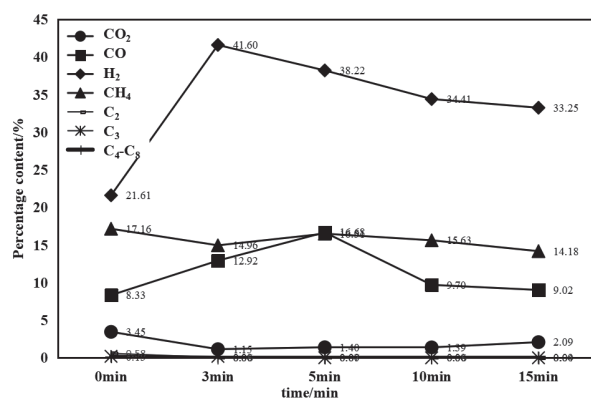


Fig. 5. Effect of constant temperature pyrolysis time on gas composition of coal pyrolysis.

Fig. 5 showed the effect of different constant temperature pyrolysis time on coal pyrolysis gas composition at a final temperature of 600°C. The detected components of pyrolysis gas were CO<sub>2</sub>, CO, H<sub>2</sub>, CH<sub>4</sub>, C<sub>2</sub>, C<sub>3</sub> and C<sub>4</sub>~C<sub>8</sub>. It can be seen from Fig. 5 that under constant temperature pyrolysis at a final temperature of 600°C, coal pyrolysis gas had the highest H<sub>2</sub> content, followed by CH<sub>4</sub> and CO content, and other gases have the lowest ratio. With the increase of the constant temperature time, the H<sub>2</sub> content first increased and then decreased, but the H<sub>2</sub> content was higher than the H<sub>2</sub> content at 0 min under different constant temperature pyrolysis time, and the H<sub>2</sub> content was the highest at 3 min of constant temperature pyrolysis, which was 41.6%. From the Fig. 4, it can be calculated that the total content of H<sub>2</sub> and CH<sub>4</sub> was 56.6% at the highest temperature for 3 min of isothermal pyrolysis; the total content of CO, H<sub>2</sub> and CH<sub>4</sub> was 71.4% for 5 min of isothermal pyrolysis. At this time, the pyrolysis gas contained higher fuel gas, so it can be used as the time point for the pyrolysis of industrial coal to prepare and collect fuel gas. It can also be seen from Fig. 5 that at the final temperature 600°C, the H<sub>2</sub> content produced by constant temperature pyrolysis was significantly higher than the H<sub>2</sub> content produced at different final temperatures, which proved that the temperature of 600°C was the third in coal pyrolysis. The production of hydrogen in the volatiles of the stage degassing was high. When coal was pyrolyzed at 600°C, it was in the secondary degassing stage of coal. At this stage, the main reaction was condensation polymerization. On the one hand, the amount of gas was released, on the other hand, the semi-coke itself increased in density and volume was contracted. The large amount of hydrogen released at this temperature is due to the relatively simple condensation of the aromatic part.

### Effect of Alkali Metal Oxidation Supported Catalyst on Coal Pyrolysis Products

Fig. 6 showed the changes of gas products and tar under the conditions of final pyrolysis temperature 600°C and constant temperature of 5 min after mixing 15 g coal sample and 3g different alkaline earth metal oxide supported  $\gamma$ -Al<sub>2</sub>O<sub>3</sub> catalyst into pyrolysis furnace. The alkaline earth metal oxides selected MgO, CaO, SrO and BaO as the active components of the catalyst, which can catalyze the pyrolysis of coal and increase the pyrolysis products. At the same time, it also played a catalytic role in the pyrolysis products of coal to increase gas production and oil and gas quality. It can be seen from Fig. 4 that the final pyrolysis temperature 600°C and the pyrolysis time 5 min, the gas quality and tar quality were 1.58 g and 0.33 g, respectively. In Fig. 6, it can be seen that the pyrolysis products of coal with catalyst have obvious changed, and the tar yield with  $\gamma$ -Al<sub>2</sub>O<sub>3</sub> and SrO/ $\gamma$ -Al<sub>2</sub>O<sub>3</sub> increased by 27.27% and 18.18% respectively compared with the tar yield

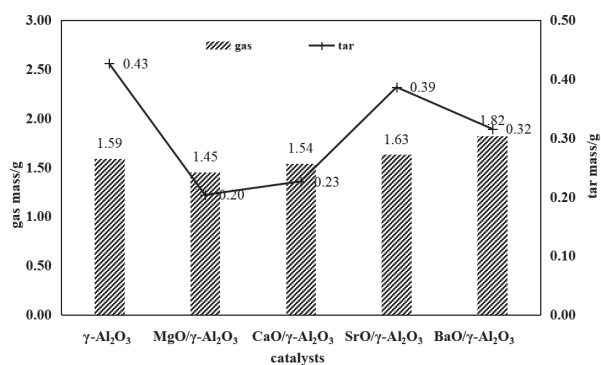


Fig. 6. Effect of alkaline earth metal oxide supported  $\gamma\text{-Al}_2\text{O}_3$  catalyst on gas and tar.

at 600°C and 5 min. BaO/ $\gamma\text{-Al}_2\text{O}_3$  was added, and the gas output was increased by 24% than that of 600°C and 5 min. Therefore, it can be concluded that  $\gamma\text{-Al}_2\text{O}_3$  and SrO/ $\gamma\text{-Al}_2\text{O}_3$  had obvious effect on the increase of tar output and BaO/ $\gamma\text{-Al}_2\text{O}_3$  had obvious effect on the gas quality of coal pyrolysis.  $\gamma\text{-Al}_2\text{O}_3$  was loaded with 5% alkaline earth metal oxide. 5% of the alkaline earth metal oxides are converted by amount of substance. It was found that the amount of MgO and CaO supported on the catalysts was large, and the pore channel of the catalysts was blocked by MgO and CaO, which reduced the catalytic effect of the catalysts. This was also proved by the characterization of specific

surface area. So the value of MgO/ $\gamma\text{-Al}_2\text{O}_3$  and CaO/ $\gamma\text{-Al}_2\text{O}_3$  was lower.

Fig. 7 was that a pyrolysis of 15 g coal mixed uniformly with 3g alkaline earth metal oxide supported  $\gamma\text{-Al}_2\text{O}_3$  catalysts in a pyrolysis furnace, Fig. 7(a-e) represent the addition of  $\gamma\text{-Al}_2\text{O}_3$ , MgO/ $\gamma\text{-Al}_2\text{O}_3$ , CaO/ $\gamma\text{-Al}_2\text{O}_3$ , SrO/ $\gamma\text{-Al}_2\text{O}_3$  and BaO/ $\gamma\text{-Al}_2\text{O}_3$ , respectively, the change of gas composition at 450°C, 500°C, 550°C, 600°C and constant temperature 5 min. It can be seen in Fig. 7 that the change trend of the gas with the pyrolysis temperature was basically the same after adding different catalysts, and the  $\text{CH}_4$  content reached the maximum when the pyrolysis temperature reached 550°C. When the pyrolysis temperature reached 600°C and the final temperature was constant temperature 5 min, the  $\text{H}_2$  content was the maximum. The content of  $\text{CH}_4$  produced by  $\gamma\text{-Al}_2\text{O}_3$  during coal pyrolysis and cracking was the highest, its value was 38.4%, and the temperature at this time was 550°C. The BaO/ $\gamma\text{-Al}_2\text{O}_3$  catalyst made the total content of CO,  $\text{H}_2$  and  $\text{CH}_4$  the highest, its value was 86.5%, and the total content of  $\text{H}_2$  and  $\text{CH}_4$  were the highest, its value was 67.7%. At this time, the pyrolysis condition was constant temperature 5 min. At the same time, the BaO/ $\gamma\text{-Al}_2\text{O}_3$  catalyst made the total content of CO,  $\text{H}_2$  and  $\text{CH}_4$  higher than 70% after pyrolysis 550°C. The catalyst prepared in this study was better than other catalysts for pyrolysis of coal [14-15], and the yields of  $\text{H}_2$  and  $\text{CH}_4$  are both higher. According to the above analysis, the BaO/ $\gamma\text{-Al}_2\text{O}_3$  catalyst had a better effect on

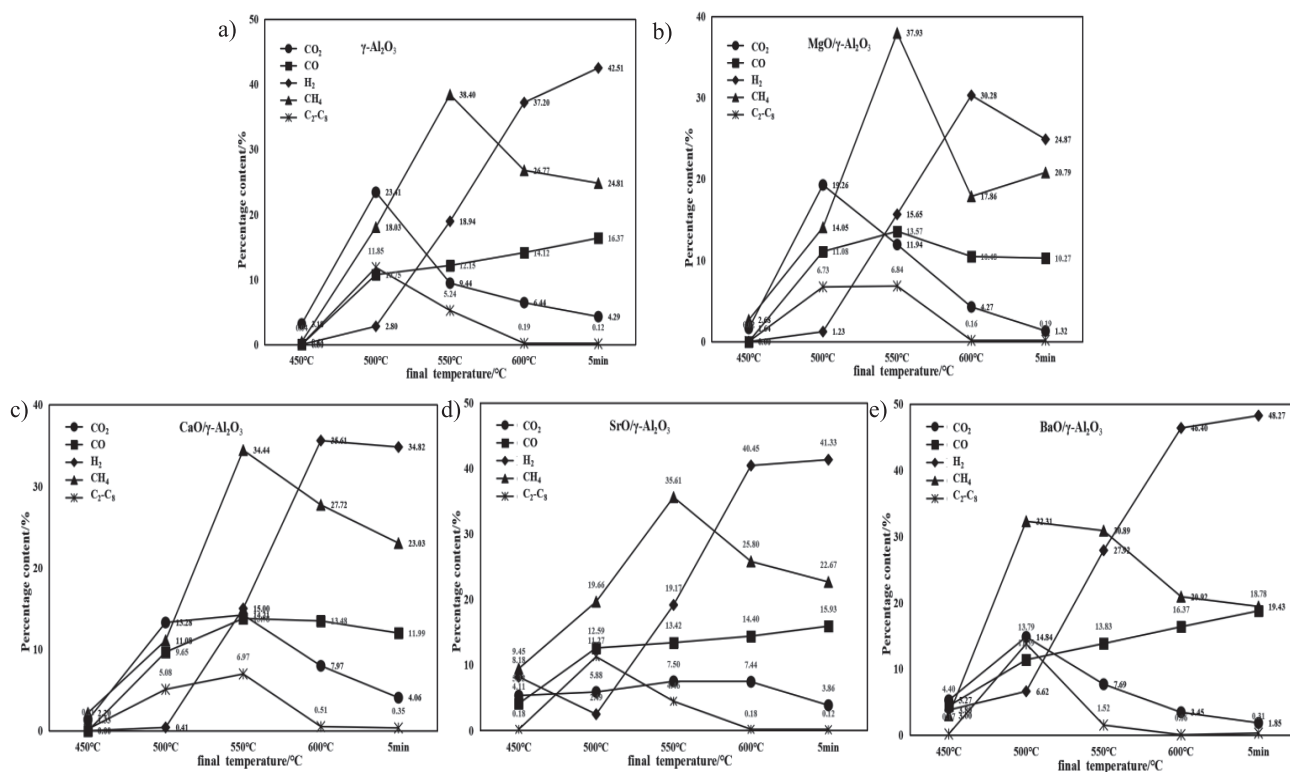


Fig. 7. effect of  $\gamma\text{-Al}_2\text{O}_3$  supported on alkaline earth metal oxide catalyst on gas components from coal pyrolysis: a)  $\gamma\text{-Al}_2\text{O}_3$ , b) MgO/ $\gamma\text{-Al}_2\text{O}_3$  catalyst, c) CaO/ $\gamma\text{-Al}_2\text{O}_3$  catalyst, d) SrO/ $\gamma\text{-Al}_2\text{O}_3$  catalyst, e) BaO/ $\gamma\text{-Al}_2\text{O}_3$  catalyst.

Table 3. Specific surface area and pore size of the catalyst.

	Specific surface area (m <sup>2</sup> /g)	Pore volume (cm <sup>3</sup> /g)	Void diameter (nm)
$\gamma$ -Al <sub>2</sub> O <sub>3</sub>	271.6418	0.450463	6.6332
MgO/ $\gamma$ -Al <sub>2</sub> O <sub>3</sub>	183.2134	0.315235	4.1246
CaO/ $\gamma$ -Al <sub>2</sub> O <sub>3</sub>	201.2462	0.362059	4.6236
SrO/ $\gamma$ -Al <sub>2</sub> O <sub>3</sub>	215.2523	0.413412	5.8013
BaO/ $\gamma$ -Al <sub>2</sub> O <sub>3</sub>	266.5736	0.432305	6.2507

the catalytic cracking of coal pyrolysis to produce hydrogen-rich fuel gas.

## Characterization

### Specific Surface Area of Catalysts

Table 3 showed the characterization results of specific surface area and pore size of different catalysts. In the process of coal pyrolysis, oil vapor molecules entered the catalyst and contacted with the active sites to produce small molecular substances. The specific surface area and pore size of the catalyst played a very important role in the catalytic cracking of oil vapor molecules. It can be seen from Table 3 that the specific surface area of  $\gamma$ -Al<sub>2</sub>O<sub>3</sub> was 271.6418 m<sup>2</sup>/g. After loading, the specific surface areas of MgO/ $\gamma$ -Al<sub>2</sub>O<sub>3</sub>, CaO/ $\gamma$ -Al<sub>2</sub>O<sub>3</sub>, SrO/ $\gamma$ -Al<sub>2</sub>O<sub>3</sub> and BaO/ $\gamma$ -Al<sub>2</sub>O<sub>3</sub> decreased. The reason was that the specific surface area of MgO/ $\gamma$ -Al<sub>2</sub>O<sub>3</sub>, CaO/ $\gamma$ -Al<sub>2</sub>O<sub>3</sub>, SrO/ $\gamma$ -Al<sub>2</sub>O<sub>3</sub> and

BaO/ $\gamma$ -Al<sub>2</sub>O<sub>3</sub> after loading was reduced, which was due to the formation of oxides after calcination of the supported catalyst, resulting in smaller specific surface area of the support [16]. However, both  $\gamma$ -Al<sub>2</sub>O<sub>3</sub> and BaO/ $\gamma$ -Al<sub>2</sub>O<sub>3</sub> had better catalytic cracking effect on coal pyrolysis because of their larger specific surface area, which can better adsorb oil and gas molecules and contact them with active sites and take place catalytic cracking reaction.

### X-ray Diffraction of Catalysts

Fig. 8 shows the XRD spectra of  $\gamma$ -Al<sub>2</sub>O<sub>3</sub>, MgO/ $\gamma$ -Al<sub>2</sub>O<sub>3</sub>, CaO/ $\gamma$ -Al<sub>2</sub>O<sub>3</sub>, SrO/ $\gamma$ -Al<sub>2</sub>O<sub>3</sub> and BaO/ $\gamma$ -Al<sub>2</sub>O<sub>3</sub>. It can be seen from Fig. 8 that the corresponding alkaline earth metal oxides were formed on the catalyst after calcination of  $\gamma$ -Al<sub>2</sub>O<sub>3</sub> impregnated with alkali metal salt in muffle furnace. In Fig. 8a), 2 $\theta$  angles of 32.78, 36.54, 37.51, 43.17, 45.79, 66.76 and 67.31 were the characteristic peaks of  $\gamma$ -Al<sub>2</sub>O<sub>3</sub> [17]. In Fig. 8b), the 2 $\theta$  angles of 29.26, 38.44, 44.37, 64.53,

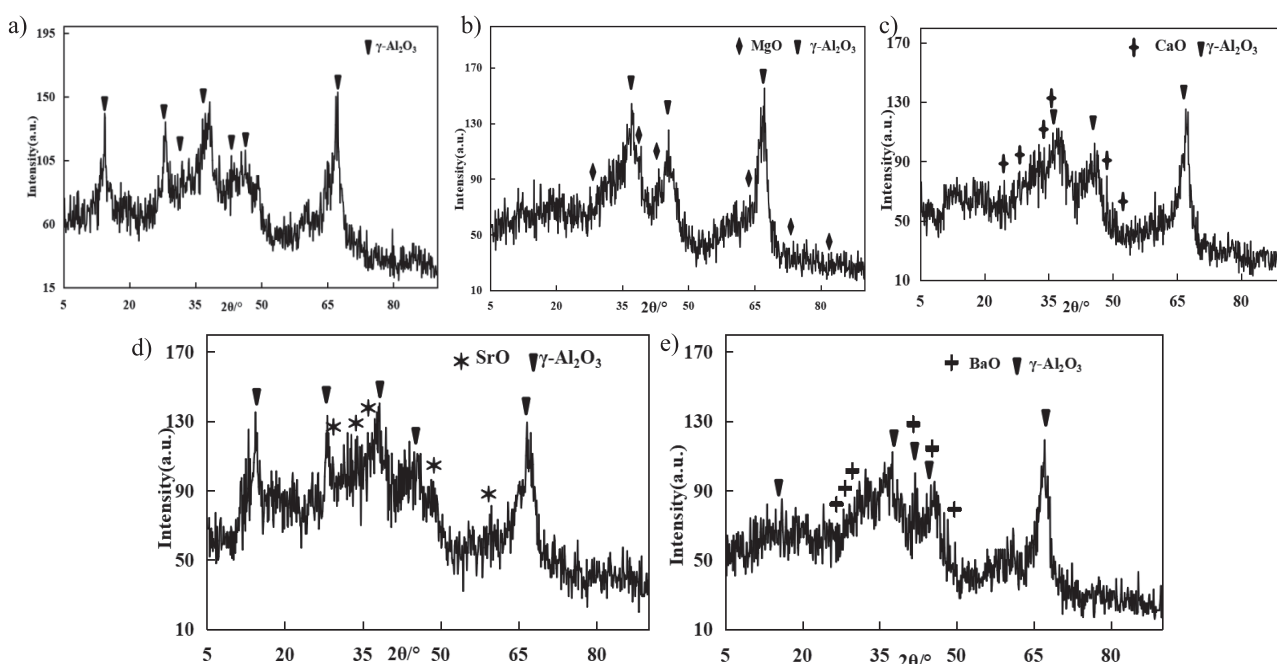


Fig. 8. XRD of alkaline earth metal oxide supported  $\gamma$ -Al<sub>2</sub>O<sub>3</sub> catalyst: a)  $\gamma$ -Al<sub>2</sub>O<sub>3</sub>, b) MgO/ $\gamma$ -Al<sub>2</sub>O<sub>3</sub> catalyst, c) CaO/ $\gamma$ -Al<sub>2</sub>O<sub>3</sub> catalyst, d) SrO/ $\gamma$ -Al<sub>2</sub>O<sub>3</sub> catalyst, e) BaO/ $\gamma$ -Al<sub>2</sub>O<sub>3</sub> catalyst.

Table 4. Alkaline earth metal content of supported  $\gamma$ -Al<sub>2</sub>O<sub>3</sub> catalysts (%).

Catalysts	MgO/ $\gamma$ -Al <sub>2</sub> O <sub>3</sub>	CaO/ $\gamma$ -Al <sub>2</sub> O <sub>3</sub>	SrO/ $\gamma$ -Al <sub>2</sub> O <sub>3</sub>	BaO/ $\gamma$ -Al <sub>2</sub> O <sub>3</sub>
Element	Mg	Ca	Sr	Ba
Theoretical content	9.00	10.71	12.69	13.43
Assay content	8.91	10.23	12.54	13.37

73.33 and 82.01 were characteristic peaks of MgO [18]. In Fig. 8c), the  $2\theta$  angles of 26.75, 29.76, 37.36 and 53.86 were the characteristic peaks of CaO [19]. In Fig. 8d), the  $2\theta$  angles of 30.00, 34.73, 36.52, 49.93 and 59.34 were the characteristic peaks of SrO [20]. In Fig. 8e), the  $2\theta$  angles of 27.88, 28.68, 31.91, 41.17, 46.53 and 48.02 are the characteristic peaks of BaO [21]. The diffraction peaks of these catalysts were strong, popular and sharp, and the oxides formed had good dispersion, which increased the catalytic activity of the catalysts. The results showed that the specific surface area of BaO/ $\gamma$ -Al<sub>2</sub>O<sub>3</sub> was smaller than that of  $\gamma$ -Al<sub>2</sub>O<sub>3</sub>, but the activity of BaO/ $\gamma$ -Al<sub>2</sub>O<sub>3</sub> catalyst was improved, and the effect of BaO/ $\gamma$ -Al<sub>2</sub>O<sub>3</sub> on coal pyrolysis was the best.

#### Determination of Alkaline Earth Metal Elements in Catalysts by Inductively Coupled Plasma Mass Spectrometer

Table 4 showed the determination of Alkali metal elements in supported catalysts. As can be seen from the Table 4, the actual and theoretical contents of alkaline earth metal elements determined by ICP-MS were almost the same, and the experimental operation can ensure that more active components can be formed on the support of the catalyst, to ensure the activity of the catalyst.

### Conclusions

The maximum tar and gas were 0.32 g and 1.44 g respectively at the final temperature of 600°C, and the optimum temperature was 600°C for coal tar pyrolysis, and the maximum content of CH<sub>4</sub> was between 450°C and 550°C, when the temperature reached 600°C, the content of H<sub>2</sub> in pyrolytic gas was the highest. Under the condition of constant temperature pyrolysis at 600°C, the content of hydrogen in pyrolysis gas was the highest, and the output of oil was basically unchanged.  $\gamma$ -Al<sub>2</sub>O<sub>3</sub> made the highest yield of coal tar and better oil production for coal pyrolysis and catalytic cracking, while SrO/ $\gamma$ -Al<sub>2</sub>O<sub>3</sub> made the highest yield of pyrolysis gas and the highest content of hydrogen-rich combustible gas, BaO/ $\gamma$ -Al<sub>2</sub>O<sub>3</sub> catalyst has a good effect on catalytic pyrolysis of coal to produce hydrogen-rich fuel gas. It was found that the specific surface areas of  $\gamma$ -Al<sub>2</sub>O<sub>3</sub> and BaO/ $\gamma$ -Al<sub>2</sub>O<sub>3</sub> were almost the same, but it was found that BaO/ $\gamma$ -Al<sub>2</sub>O<sub>3</sub> catalysts contained more

active components by XRD characterization, therefore, BaO/ $\gamma$ -Al<sub>2</sub>O<sub>3</sub> has better catalytic cracking effect.

### Acknowledgments

Financial support of this research was provided by Key Laboratory of Coal Resources Exploration and Comprehensive Utilization, Ministry of Land and Resources (Program No.KF2020-10) in P.R. China. The Key Industry Chain Innovation Project, Shaanxi province, China (2018GY-076).

### Conflict of Interest

The authors declare no conflict of interest.

### Reference

- GUO H.Y., ZHAO S.F., DONG Z.W., WANG Q., XIA D.P., JIA J.B., YIN X.J., YU H.F. Clean and efficient utilization of coal combined with corn straw by synergistic biodegradation. *Renewable Energy*, **161**, 701, **2020**.
- WU J., DI Z.X., LUO M.S., WANG Y.T., DING X.X., LI H.J. Current Situation and Research Progress of Coal Pyrolysis Technology. *Coal Chemical Industry*, **47** (6), 46, **2019**.
- HU D.D., ZENG X., WANG F., HAN Z.N., DING F., YUE J.R., XU G.W. Release behavior and generation kinetics of gas product during rice husk pyrolysis in a micro spouted bed reactor. *Fuel*, **287**, 1, **2021**.
- SUN H.Y., YANG Q., FAN J.L. Development status and trend analysis of Xinjiang coal and coal chemical industry. *Coal Economic Research*, **40** (2), 57, **2020**.
- CHEN J.H., LI Y., CHEN X.J., ZHANG L., YANG D.F. Study on calorific value of semi-coke and desulfurization effect during pyrolysis of bituminous coal. *Fresenius Environmental Bulletin*, **30** (05), 4756, **2021**.
- XU Y., LUO G.Q., ZHANG Q.Z., LI Z.H., ZHANG S.B., CUI W. Cost-effective sulfurized sorbents derived from one-step pyrolysis of wood and scrap tire for elemental mercury removal from flue gas. *Fuel*, **285**, 1, **2021**.
- KIM H., KIM B., LIM H., SOMG J. Effect of liquid carbon dioxide on coal pyrolysis and gasification behavior at subcritical pressure conditions. *Chemical Engineering Science*, **231**, 1, **2021**.
- RICHARD A.P., JOHNSON C., FLETCHER T.H. Correlations of the Elemental Compositions of Primary Coal Tar and Char. *Energy & Fuels*, **33** (10), 9520, **2019**.
- CHEN J.H., LI Y., CHEN X.J., ZHANG L., YANG D. Study on calorific value of semi-coke and desulfurization



- effect during pyrolysis of bituminous coal. *Fresenius Environmental Bulletin*, **30**, 4756, **2021**.
10. LIU S.C., FU X.M., ZHU F.H., IA J.W., LI N., GAO C.L. XU J.Q., SHU X.Q. Catalytic pyrolysis of coking-coal tailings for production of hydrogen-rich fuel gas. *Chinese Journal of Environmental Engineering*, **7** (10), 4067, **2013**.
  11. ZHAO H.Y., LI Y.H., SHU Y.F., SONG Q., LYU J.X., WANG Z.M. ZENG M., SHU X.Q. Effect of calcium oxide on pyrolysis product distribution and char structure of lignite and anthracite. *Coal Science and Technology*, **44** (3), 177, **2016**.
  12. JIAO Y., WANG J., QIN L.X., WANG J.L., ZHU Q., LI X.Y., GONG M.C., CHEN Y.Q. Kerosene cracking over supported monolithic Pt catalysts, Effects of SrO and BaO promoters. *Chinese Journal of Catalysis*, **34** (6), 1139, **2013**.
  13. WANG D., MA S.W., XIANG W.G., CHEN S.Y. Pyrolysis characteristics of ash-free Xuzhou bituminous coal with Fe/CaO catalyst. *Chemical Industry and Engineering Progress*, **39** (2), 561, **2020**.
  14. ZHANG L., CHANG X., CHEN J.H., LEI Z., MA Z.H., WEN X., YANG C., JIA Y. Preparation of NiO/PC catalyst with plasma for cracking tar to produce flammable gas. *International Journal of Hydrogen Energy*, **45** (21), 12000, **2020**.
  15. ZHANG P.W., WANG B., TIAN W.D., YANG S.Y., XIAO Y.H. Influences of mixing methods on CaO/char steam gasification. *Journal of China Coal Society*, **41** (8), 2097, **2016**.
  16. LIU Y.W., QUAN X., CHEN S., YU H.T., DU L. Catalytic wet peroxide oxidation for organic wastewater treatment by  $\text{Fe}_2\text{O}_3/\text{Al}_2\text{O}_3$  catalyst coupled with membrane. *Journal of Dalian University of Technology*, **59** (6), 587, **2019**.
  17. CHEN Y., LIU T.C., GAO Y.H., GAO Y.H., LIANG Y.N. In situ co-precipitation of NiMg (Al)O on  $\gamma\text{-Al}_2\text{O}_3$  and its catalytic performance in the transesterification. *Journal of Fuel Chemistry and Technology*, **46** (1), 59, **2018**.
  18. WANG S.H., ZHU D.C., SHAO J.A., XIANG J.T., YANG H.P., YI J., ZHANG S.H., CHEN H.P. Preparation of MgO Modified Lotus Shell Biochar and Its Phosphorus Adsorption Characteristics. *Environmental Science*, **40** (11), 4987, **2019**.
  19. LIN Y.Y., ZHANG C., ZHU L.T., XU Z.W., GU M.Y., CHU H.Q. Experimental study on pyrolysis of camphor wood catalyzed by CaO-calcined phosphate mixtur. *Petrochemical Technology*, **288**, 1, **2021**.
  20. PALITSAKUN S., KOONKUER K., TOPOOL B., SEUBSAI A., SUDSAKORN K. Transesterification of Jatropha oil to biodiesel using SrO catalysts modified with CaO from waste eggshell. *Catalysis Communications*, **149**, 1, **2021**.
  21. ZAKALY HESHAM M.H., SAUDI H.A., ISSA SHAMS A.M., RASHAD M., ELAZAKA A.I., TEKIN H.O., SADDEEK Y.B. Alteration of optical, structural, mechanical durability and nuclear radiation attenuation properties of barium borosilicate glasses through BaO reinforcement, Experimental and numerical analyses. *Ceramics International*, **47** (4), 5587, **2021**.